Absolute Configuration of Verticillane Diterpenoids by Vibrational Circular Dichroism

Carlos M. Cerda-García-Rojas,*,† Hugo A. García-Gutiérrez,† Juan D. Hernández-Hernández,‡ Luisa U. Román-Marín,‡ and Pedro Joseph-Nathan†

Departamento de Química, Centro de Investigación y de Estudios Avanzados del Instituto Politécnico Nacional, Apartado 14-740, México, D. F., 07000 Mexico, and Instituto de Investigaciones Químico-Biológicas, Universidad Michoacana de San Nicolás de Hidalgo, Apartado 137, Morelia, Michoacán, 58000 Mexico

Received November 30, 2006

Good agreement between theoretical and experimental vibrational circular dichroism curves of (1*S*,11*S*,12*S*)-(+)-verticilla-3*E*,7*E*-dien-12-ol (**1**) established the absolute configuration of this natural diterpene isolated from *Bursera suntui*. Molecular modeling of **1** was carried out using the Monte Carlo protocol followed by geometry optimization at the B3LYP 6-31G(d,p) level of theory. The 12-membered ring of **1** was found in a single preferred chair−chair−chair−chair conformation. In the six-membered ring a chair prevails over a distorted boat, and the C−OH bond rotation generates three predominant rotamers. Validation of the minimum energy conformation for **1** was achieved by comparison of theoretical and experimental infrared frequencies, vicinal ^{1}H NMR coupling constants, and X-ray diffraction data. This study confirms that (+)-verticillol **1** isolated from *Bursera* species has the 1*S*,11*S*,12*S* absolute configuration that corresponds to the same enantiomeric series as verticillanes from *Sciadopitys* and *Taxus*, while verticillanes from *Jackiella* and *Jungermannia* have antipodal structures.

Verticillane diterpenoids have recently attracted the attention of natural product chemists due to their fundamental role in the biosynthesis of taxanes. It has been demonstrated that the cyclization mechanism from (*E*,*E*,*E*)-geranylgeranyl diphosphate to taxa-4,11-diene proceeds through a verticillen-12-yl carbocation intermediate.[1] Some hydroxylated verticillane derivatives have been isolated from diverse sources such as the conifer *Sciadopitys verticillata*,[2] the dicotyledons *Bursera suntui* and *B. kerberi*,[3] the soft coral *Cespitularia hypotentaculata*,[4] and the liverworts *Jackiella javanica* and *Jungermannia infusca*.[5,6] Several polyfunctionalized derivatives of this bicyclic diterpene have also been isolated from *Taxus* species. Taxuspine X possesses a potent multidrug-resistance reversing activity.[7]

By analyzing the biogenetic relationships and optical activity data of verticillane derivatives isolated from several sources, it could be predicted that their absolute configuration should be reversed. The absolute configuration of (+)-verticillol from *Sciadopitys verticillata* was studied by anomalous dispersion X-ray analysis of its derived *p*-iodobenzoate,[1] from which it was concluded that indeed the absolute configuration of all verticillanes previously described required revision. However, in a recent article on *ent*-(−)-verticillene derivatives from *Jackiella javanica*,[6] the authors maintain the absolute configuration as originally proposed from the octant rule analysis of a nor-ketodiepoxide derivative. In view of this controversy, and due to the relevance of an unequivocal definition of the absolute configuration of verticillane derivatives, we ventured to confirm this stereochemical feature using an independent methodology and also to rationalize the origin of the discrepancy. In this context, comparison of theoretical and experimental vibrational circular dichroism (VCD) spectra has been used recently to determine the absolute configuration of chiral molecules.[8−14] Remarkable improvements in computer systems and software developments have recently allowed organic chemists to apply this methodology to relatively complex molecules, including natural products.[15−19] Therefore in this work we contrast the experimental VCD spectrum of (+)-verticillol **1** (Scheme 1), isolated from *Bursera suntui*,[3] with the theoretical curve obtained by calculation of all significantly populated conformations using density functional theory (DFT)[20] calculation of the VCD frequencies and generation of the weighted-averaged vibrational plot.

Scheme 1. Verticillanes **1**−**7** and Norketodiepoxide **8**

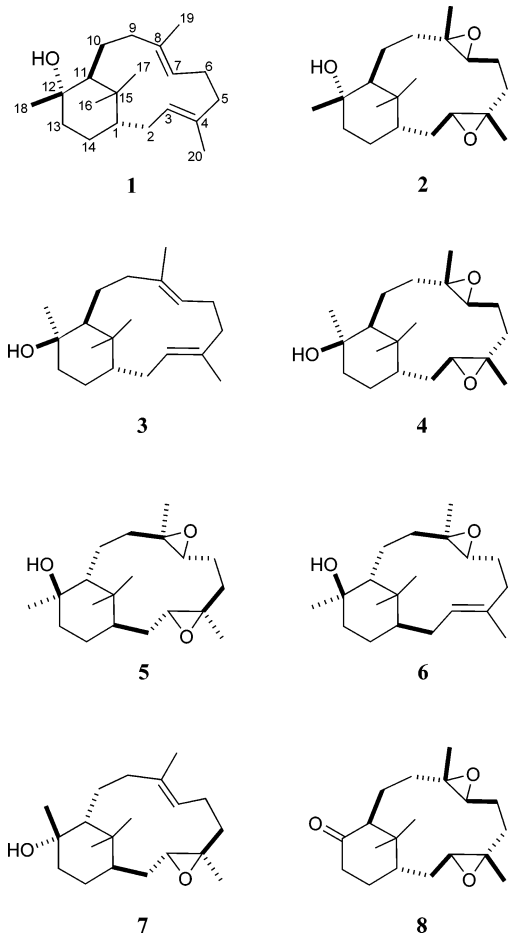

Results and Discussion

(+)-Verticillol **1** was obtained from the stems of *B. suntui* as previously described.[3] Its VCD spectrum, measured from a CCl_4

* To whom correspondence should be addressed. Tel: +52 55 5747 7112. Fax: +52 55 5747 7137. E-mail: ccerda@cinvestav.mx.
† Centro de Investigación y de Estudios Avanzados del Instituto Politécnico Nacional.
‡ Universidad Michoacana de San Nicolás de Hidalgo.

10.1021/np0605992 CCC: $37.00
Published on Web 06/21/2007

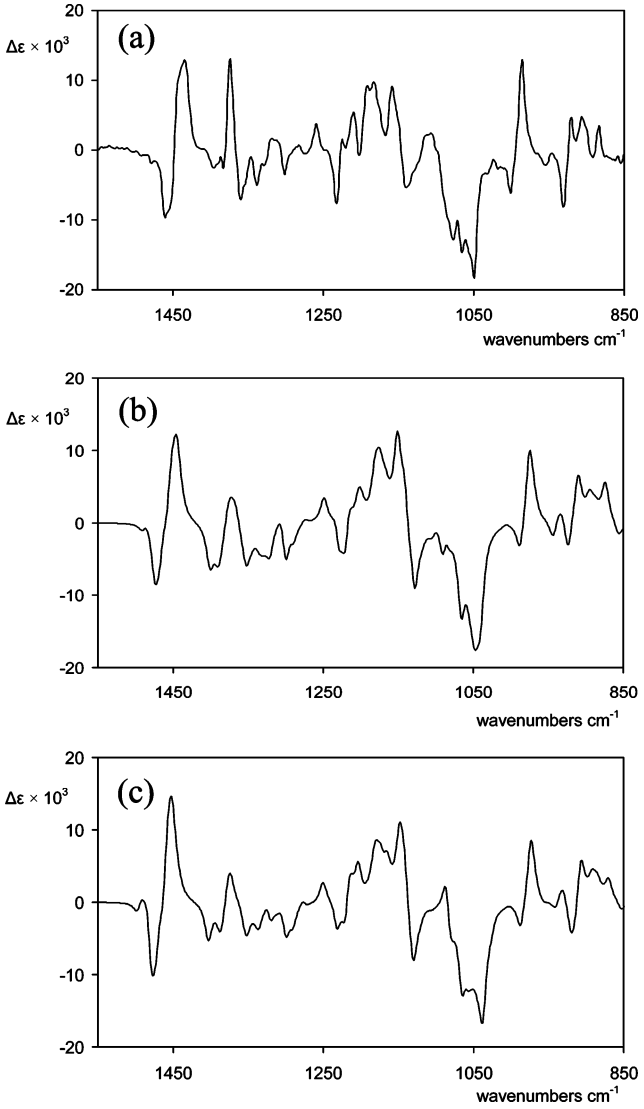

Figure 1. (a) Experimental VCD spectrum of (+)-verticillol (**1**) isolated from *B. suntui*; (b) B3LYP/6-31G(d,p) DFT and (c) B3LYP/DGDZVP DFT Boltzmann-weighted VCD spectra of (1*S*,11*S*,12*S*)-verticilla-3*E*,7*E*-dien-12-ol (**1**).

solution, is depicted in Figure 1a and is compared with the Boltzmann-weighted theoretical curve of (1*S*,11*S*,12*S*)-verticilla-3*E*,7*E*-dien-12-ol (**1**) calculated at the DFT B3LYP/6-31G(d,p) and B3LYP/DGDZVP levels of theory shown in Figure 1b and 1c, respectively. The comparison establishes that natural (+)-verticillol **1** has the absolute configuration depicted in Scheme 1 in accordance with the proposed modification based on X-ray diffraction analysis of (+)-verticillol *p*-iodobenzoate[1] and in disagreement with the absolute configuration proposed on the basis of the octant rule.[2,5,6]

The theoretical VCD spectrum of (1*S*,11*S*,12*S*)-verticilla-3*E*,7*E*-dien-12-ol (**1**) was obtained employing a molecular modeling protocol that initially involved the use of systematic and Monte Carlo conformational searching methods. The (1*S*,11*S*,12*S*)-verticilla-3*E*,7*E*-dien-12-ol (**1**) model was constructed starting from the minimized 12-membered ring followed by consecutive incorporation of the six-membered ring, the methyl groups, and the hydroxy group. In each step a full minimization routine employing molecular mechanics (MMFF) was carried out. In this process the energy value was monitored as a convergence criterion to yield the global minimum energy structure at $E_{MMFF} = 87.885$ kcal/mol. The Monte Carlo search using the global minimum as the starting point afforded a total of six conformational species arising from two different conformations at the six-membered ring and three rotamers with

Table 1. Molecular Mechanics Relative Energy, Molecular Mechanics Population, DFT Thermochemical Parameters, and DFT Population for the Six Minimum Energy Structures of (1*S*,11*S*,12*S*)-Verticilla-3*E*,7*E*-dien-12-ol (**1**)

conformer	ΔE_{MMFF}[a]	p_{MMFF}[b]	ΔE_0[c,d]	ΔE_{298}[d]	ΔH_{298}[d]	ΔG_{298}[d]	p_{DFT}[e]
1a	0.000	61.59	0.000	0.000	0.000	0.000	42.50
1b	0.475	27.84	−0.051	−0.078	−0.078	0.045	39.39
1c	1.059	10.39	0.465	0.419	0.420	0.617	15.00
1d	3.730	0.11	3.020	3.116	3.116	2.291	0.89
1e	4.280	0.05	2.364	2.412	2.412	1.831	1.92
1f	4.697	0.02	3.622	3.735	3.735	2.935	0.30

[a] Molecular mechanics energy of conformers obtained from the Monte Carlo analysis, in kcal/mol relative to **1a** with $E_{MMFF} = 87.885$ kcal/mol. [b] Molecular mechanics population in %. [c] Sum of electronic and zero-point DFT/B3LYP/6-31G(d,p) energies in kcal/mol relative to conformer **1a** calculated at 298 K and 1 atm. [d] For structure **1a** the absolute values are $E_0 = -857.336809$ au, $E_{298} = -857.314522$ au, $E_{298} + H_{298} = -857.313578$ au, $G_{298} = -857.384480$ au. [e] DFT population in % calculated from ΔG_{298} values.

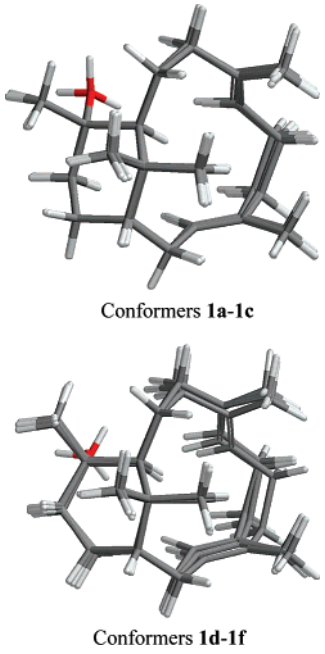

Figure 2. Superimposed molecular mechanics minimum energy structures of **1**. For details see Table 1.

three different C11−C12−O12−H dihedral angles (Table 1). The superimposed structures of the three rotamers corresponding to each conformation, whose energy values corresponded to $E_{MMFF} =$ 87.885, 88.360, 88.944, 91.615, 92.166, and 92.582 kcal/mol, are illustrated in Figure 2. The structures were submitted to geometry optimization using DFT calculations[20] at the B3LYP/6-31G(d,p) level of theory to obtain an accurate molecular model of the macrocyclic diterpene. Table 1 summarizes the thermochemical parameters for the estimation of the population of each species, which was calculated according to the $\Delta G = \Delta H - T\Delta S$ and $\Delta G = -RT \ln K$ equations, considering the B3LYP/6-31G(d,p)-calculated frequencies at 298 K and 1 atm. It was found that the hydrocarbon framework of the three lower-energy conformations (**1a**−**1c**) of (1*S*,11*S*,12*S*)-verticilla-3*E*,7*E*-dien-12-ol (Table 1), which account for ca. 97% of the DFT population, essentially maintained the same ring conformation. The very close spatial arrangement was evident from the dihedral angles listed in Table 2. In these three conformations (**1a**−**1c**) the six-membered ring exists in a chair conformation and the cyclododecadiene moiety is in a distorted chair−chair−chair−chair conformation.[21,22] The main difference resides in the C11−C12−O12−H dihedral angle, with values of +51.6° for **1a**, +170.9° for **1b**, and −74.5° for **1c**, whose variation slightly modified the hydrocarbon skeleton. In turn, higher-

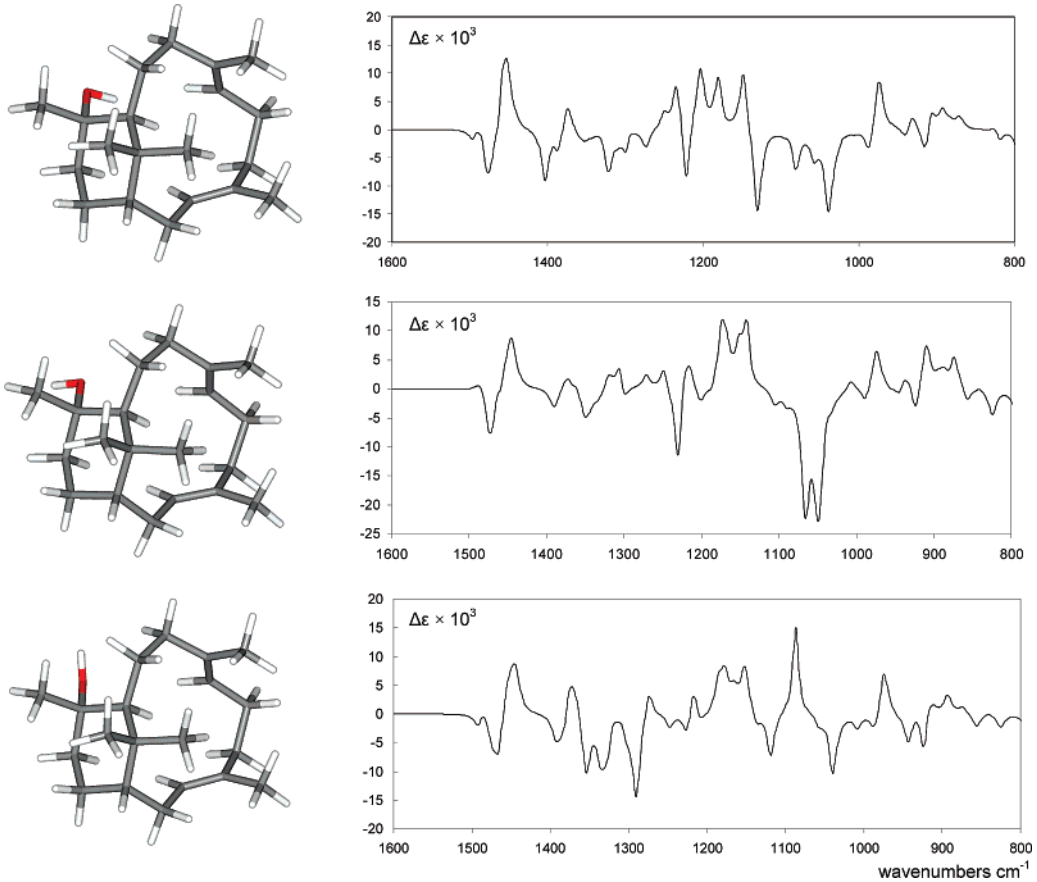

Figure 3. DFT molecular models at the B3LYP/6-31G(d,p) level of theory for the three lower-energy hydroxy group rotameric species of **1** and their corresponding VCD spectra. Lorentzian curves with 6 cm^{-1} bandwidth.

Table 2. Torsion Angles (in deg) for the 12-Membered Ring of Verticillanes **1**, **2**, and **4** and *ent*-Verticillanes **5**−**7**

torsion angle	**1a**[a]	**1b**[a]	**1c**[a]	**2**[b]	**4**[b]	**5a**[b,c]	**5b**[b,c]	**6**[b]	**7**[b]
C1−C2−C3−C4	+124.9	+125.0	+125.8	+123.3	+121.5	−120.6	−123.9	−119.6	−124.7
C2−C3−C4−C5	−178.2	−178.1	−178.1	−166.4	−163.4	+163.8	+163.6	+179.6	+164.3
C3−C4−C5−C6	+107.6	+107.0	+106.3	+104.4	+95.7	−114.0	−101.8	−115.0	−99.9
C4−C5−C6−C7	−64.1	−63.4	−63.6	−75.3	−79.6	+75.2	+76.8	+68.3	+70.1
C5−C6−C7−C8	+120.6	+122.8	+123.1	+124.7	+138.4	−117.6	−129.8	−117.4	−129.2
C6−C7−C8−C9	−173.7	−174.7	−175.1	−161.1	−159.4	+159.2	+159.7	+160.2	+176.6
C7−C8−C9−C10	+101.7	+99.7	+100.2	+99.3	+93.1	−98.5	−94.1	−97.8	−102.1
C8−C9−C10−C11	−60.0	−60.2	−60.3	−66.2	−67.4	+64.1	+66.2	+64.6	+60.6
C9−C10−C11−C15	+135.6	+136.7	+135.0	+139.4	+133.6	−148.1	−140.4	−145.4	−130.4
C10−C11−C15−C1	−173.4	−173.6	−173.2	−176.9	−178.7	+176.6	+175.6	+175.0	+174.7
C11−C15−C1−C2	+81.7	+81.5	+82.5	+80.4	+83.3	−78.1	−81.7	−78.2	−83.3
C15−C1−C2−C3	−56.6	−56.8	−56.9	−58.1	−49.6	+65.6	+59.4	+74.6	+57.1

[a] Measured in the DFT B3LYP/6-31(d,p) molecular models. [b]From X-ray diffraction analysis. [c]The asymmetric unit of the crystal cell contains two molecules.

energy conformers **1d**−**1f** (Table 1), which account for ca. 3% of the DFT population, basically displayed the same ring conformation for the cyclododecadiene moiety, but the six-membered ring adopted a boat conformation in which the C11−C12−O12−H dihedral angles were +59.0° for **1d**, −175.2° for **1e**, and −63.5° for **1f**. In the same calculation process, the infrared frequencies and the VCD frequencies were obtained for the six conformations. Evaluation of data listed in Table 1 allowed us to set up a threshold for the VCD theoretical analysis. We consider that the influence of the three low-populated conformations (ca. 3%) in the VCD theoretical curve can be neglected. The individual VCD and IR spectra of **1a**−**1c** were scaled by a factor of 0.97 as recommended[8] when using the B3LYP/6-31G(d,p) level of theory. The three low-energy minimized structures, together with the individual VCD graphics, are depicted in Figure 3, where band shapes are Lorentzian and bandwidths are 6 cm^{-1}. The strong bands within the 1200−1000 cm^{-1} region, involving the C12−O12 bond stretching, are very different in the three spectra of Figure 3, while the two bands close to 1475 and 1450 cm^{-1}, corresponding to methylene and methyl group deformations, are very similar. The three spectra were combined according to the molar fraction of each rotameric species to provide the weighted-averaged spectrum shown in Figure 1b.

Comparison of experimental and DFT B3LYP/6-31G(d,p) VCD curves shows good agreement. Quantitative evaluation of this correspondence was achieved by contrasting the theoretical versus experimental absorbance as shown in Figure 4. The very good compliance is probably due to the lack of significant electronic effects in diterpene **1** and the prevalence of a consistent conformational arrangement in the hydrocarbon framework. The matching curves indicate that the B3LYP/6-31G(d,p) basis set seems to be appropriate for this kind of molecule, in agreement with several reports,[16,18,23] which state that the B3LYP/6-31G(d,p) level of theory offers an appropriate balance between computing time and spectral

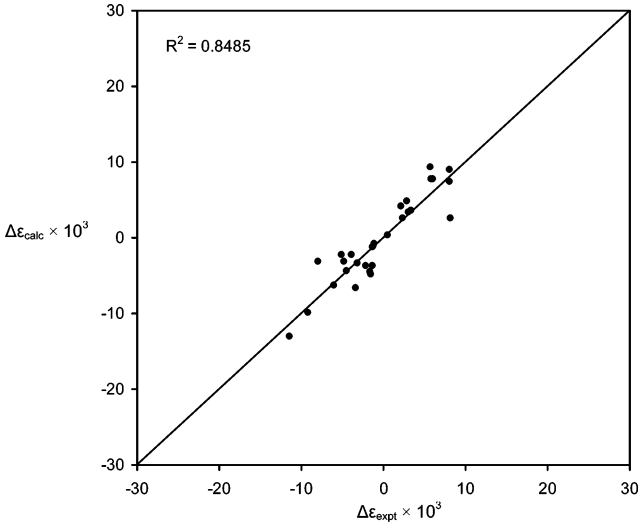

Figure 4. Comparison of experimental and B3LYP/6-31G(d,p) DFT-calculated VCD ($\Delta\epsilon$) for (1*S*,11*S*,12*S*)-(+)-verticilla-3*E*,7*E*-dien-12-ol (**1**).

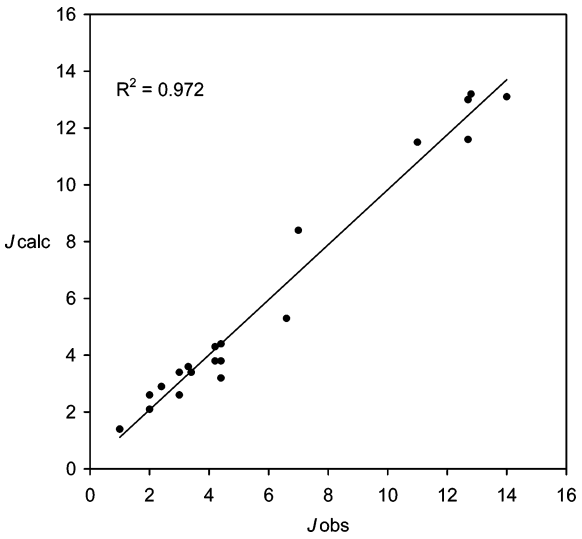

Figure 5. Comparison of observed and calculated vicinal ^{1}H NMR coupling constants for **1**.

similarity. In order to explore variations using higher computing levels, we extended calculations to the B3LYP/DGDZVP DFT level of theory, affording a theoretical VCD curve (Figure 1c) that was essentially similar to that shown in Figure 1b.

The unambiguous conformational definition of a molecule is one of the crucial issues for the success of VCD spectroscopy. Therefore, the conformation of the hydrocarbon skeleton of (1*S*,11*S*,12*S*)-verticilla-3*E*,7*E*-dien-12-ol (**1**) was validated by comparison of the experimental[3] and calculated vicinal ^{1}H NMR coupling constant values, as observed in the linear correlation shown in Figure 5. The individual coupling constants for conformers **1a**−**1c** were obtained from the corresponding DFT dihedral angles by using the Altona equation.[24,25] Each coupling constant value was Boltzmann-weighted taking into account the DFT population listed in Table 1 to integrate the population-weighted average coupling constants as done previously.[26] The good correlation between the two sets of NMR parameters indicated that the conformation of **1** in $CHCl_3$ solution is quite similar to that found in the DFT molecular models.

An analysis of the published X-ray diffraction structures of (1*S*,3*S*,4*S*,7*S*,8*S*,11*S*,12*S*)-(+)-3,4:7,8-diepoxiverticillan-12-ol (**2**),[2,27] (1*R*,3*R*,4*R*,7*R*,8*R*,11*R*,12*R*)-(−)-3,4:7,8-diepoxiverticillan-12-ol (**5**),[5,27] (1*R*,7*R*,8*R*,11*R*,12*R*)-(−)-7,8-epoxiverticill-3*E*-en-12-ol (**6**),[5,27] and

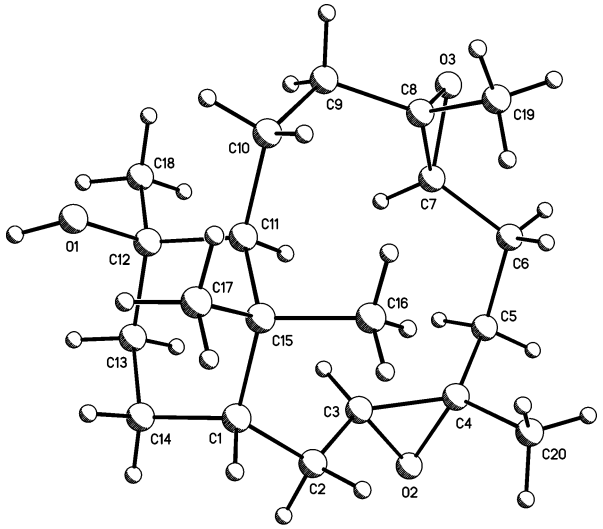

Figure 6. X-ray diffraction structure of (1*S*,3*S*,4*S*,7*S*,8*S*,11*S*,12*R*)-(+)-3,4:7,8-diepoxiverticillan-12-ol (**4**).

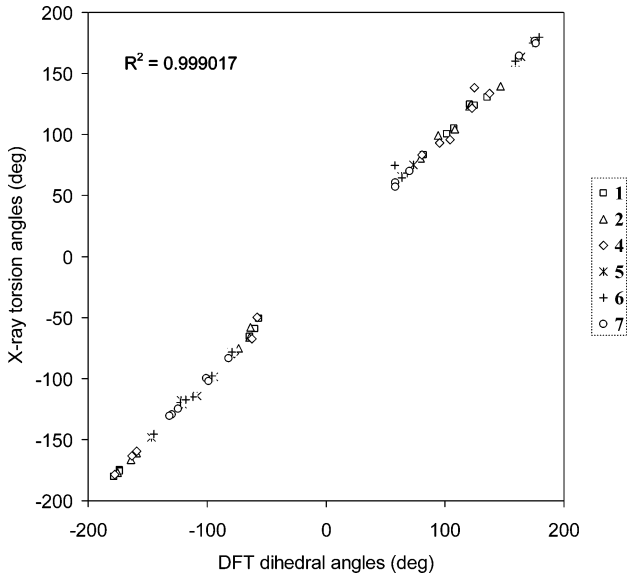

Figure 7. Comparison of DFT-calculated and X-ray torsion angles for **1**, **2**, and **4**−**7**. DFT dihedral angles of **1** are contrasted with X-ray torsion angles of its *p*-iodobenzoate derivative (ref 1). DFT dihedral angles of **5** are compared to the torsion angles of molecule **5a** (Table 2).

(1*R*,3*R*,4*R*,11*R*,12*S*)-(−)-3,4-epoxiverticill-7*E*-en-12-ol (**7**),[5,27] together with the X-ray structure of (1*S*,3*S*,4*S*,7*S*,8*S*,11*S*,12*R*)-(+)-3,4:7,8-diepoxiverticillan-12-ol (**4**) (Figure 6) determined in this work, shows that the carbocyclic system of the series exhibits the same spatial arrangement as observed in solution and in molecular models, thus generating a self-consistent picture for the preferred conformation of these compounds. Figure 7 illustrates the good agreement between DFT-calculated and X-ray torsion angles. Diepoxide **4** was obtained in good yields (81%) by treatment of verticillol **3** with hydrogen peroxide and selenium dioxide in Bu^t-OH.

The original publication on the stereochemistry of (+)-verticillol **1** described the application of the octant rule to ketone **8** for the absolute configuration determination of the natural product isolated from *Sciadopytis verticillata*.[2] In order to understand the reasoning that led to assignment of the opposite absolute configuration for (+)-verticillol **1**, the molecular model of **8** was calculated as shown in Figure 8. The work published in 1978 states that "the main contribution to the Cotton effect derives from the 12-membered ring with its substituents situated in the rear positive octant. The

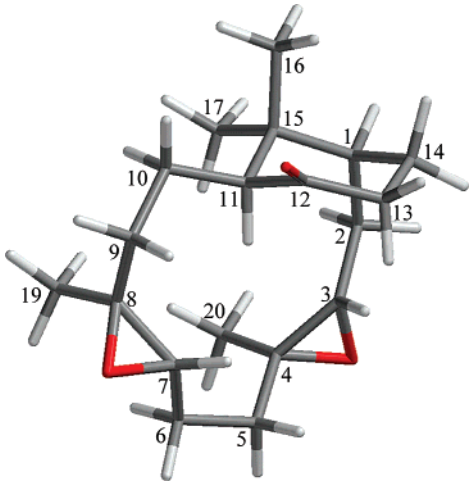

Figure 8. Molecular model for norketodiepoxide **8**.

gem-dimethyl group will have a weak designate behavior and will make no significant contribution to the observed CD."[2] However, subsequent contributions to the octant rule demonstrated that the XY surface of the octant was convex instead of planar and cutting behind the carbonyl carbon and bending outward in the +Z direction,[28,29] although the influence and the magnitude of the bending have not been completely clarified. Under these circumstances it is not certain if the C7, C8, C9, C19, and O7 atoms reside in back octants (Figure 8). If these atoms are located in the front-left-lower octant as in the classical octant system and the contribution of the axially oriented methyl group C-16 is not ignored, then the positive sign for the Cotton effect at 292 nm of this macrocyclic compound[2] can perfectly be assigned to the stereostructure drawn in Figure 8, instead of to the previously proposed enantiomeric structure.[2] This consideration eliminates the contradiction and creates consistency with the results provided by VCD analysis of (1*S*,11*S*,12*S*)-verticilla-3*E*,7*E*-dien-12-ol (**1**) reported in this work and the X-ray diffraction analysis of (+)-verticillol *p*-iodobenzoate.[1] In order to confirm this argument, the electronic circular dichroism of norketodiepoxide **8** was calculated using TDDFT methodology at the B3LYP/6-31G(d,p) level of theory. Considering the 1*S*,3*S*,4*S*,7*S*,8*S*,11*S*,12*S* absolute configuration of **8**, the predicted value for the ketone $n \rightarrow \pi^*$ transition has a positive rotatory strength at $\lambda = 291.34$ nm of $R_{velocity} = 6.8798 \times 10^{-40}$ erg·esu·cm·Gauss^{-1} and an approximate calculated[30] molecular ellipticity of $\theta_{291} = +5410$, in agreement with the reported[2] positive experimental value of $\theta_{292} = +5240$ deg·cm^2·dmol^{-1}. The calculated molecular ellipticity was obtained from the theoretical rotational strength by application of equations $R_0 \approx 0.696 \times 10^{-42}(\pi)^{1/2}3300(\Delta\epsilon^{max})(\Delta_\lambda/\lambda^{max})$ and $\theta = 3300\Delta\epsilon^{max}$, assuming that the circular dichroism curve had a Gaussian shape and considering a Δ_l value of 30 nm.[30] Furthermore, the optical rotations at the sodium D-line for verticillane derivatives **1**−**7** and norketodiepoxide **8** were calculated using the B3LYP/6-31G(d,p) DFT methods.[31] The results are summarized in Table 3, where they are compared with available literature data. These calculations, together with the VCD results, provide convincing evidence for reversing the absolute configuration. However, VCD spectroscopy has some advantages over optical rotation and electronic circular dichroism methods. VCD affords multiple data for the determination of the absolute configuration of organic molecules, in contrast to optical rotations, which are usually reported as single-parameter measurements. In VCD spectroscopy, only the electronic ground state plays a fundamental role, in contrast to electronic CD, which in addition involves participation of excited states.

It can be concluded that, nowadays, VCD spectroscopy can be efficiently applied to solve stereochemical problems in the natural products field that were difficult to settle by electronic CD,[18] as is demonstrated herein for (+)-verticillol **1**. The agreement between the theoretical and experimental VCD curves of this compound allowed us to assign its absolute configuration as 1*S*,11*S*,12*S*.

Table 3. Experimental and Calculated Specific Rotations of Verticillanes **1**−**7** and Norketodiepoxide **8**

compd	SD[a]	$[\alpha]_D$(expt)[b]	$[\alpha]_D$(calc)[b,c]	Δ_1[d]	Δ_2[e]
1	1*S*,11*S*,12*S*	+168[f]	+105.2	62.8	+273.2
2	1*S*,3*S*,4*S*,7*S*,8*S*,11*S*,12*S*	+69[g]	+77.9	−8.9	+146.9
3	1*S*,11*S*,12*R*	+149[h]	+112.0	+37.0	+261.0
4	1*S*,3*S*,4*S*,7*S*,8*S*,11*S*,12*R*	+36[i]	+47.2	−11.2	+83.2
5	1*R*,3*R*,4*R*,7*R*,8*R*,11*R*,12*R*	−98[j]	−77.9	−20.1	−175.9
6	1*R*,7*R*,8*R*,11*R*,12*R*	−114[k]	−101.1	−12.9	−215.1
7	1*R*,3*R*,4*R*,11*R*,12*S*	−48[l]	−66.9	18.9	−114.9
8	1*S*,3*S*,4*S*,7*S*,8*S*,11*S*,12*S*	+59[m]	+81.1	−22.1	+140.1

[a] Stereochemical descriptors. [b] $[\alpha]_D$ in deg·[dm·g/cm^3]$^{-1}$. [c] With B3LYP/6-31G(d,p) DFT. [d] $\Delta_1 = [\alpha]_D$(expt) − $[\alpha]_D$(calc). [e] $\Delta_2 = [\alpha]_D$(expt) − $[\alpha]_D$(calc for the enantiomer). [f] Ref 2, *c* 1.5, $CHCl_3$. [g] Ref 2, *c* 1.5, $CHCl_3$. [h] Ref 3, *c* 0.2, $CHCl_3$. [i] This work, *c* 1.05, $CHCl_3$. [j] Ref 6, *c* 0.87, $CHCl_3$. [k] Ref 6, *c* 1.81, $CHCl_3$. [l] Ref 6, *c* 0.33, $CHCl_3$. [m] Ref 2, *c* 0.15, $CHCl_3$.

Experimental Section

General Experimental Procedures. The melting point was determined on a Fisher-Johns apparatus and is uncorrected. Optical rotations were measured in $CHCl_3$ at 25 °C on a Perkin-Elmer 341 polarimeter. 1D and 2D NMR spectra were measured from $CDCl_3$ solutions containing TMS as the internal standard at 300 MHz for ^{1}H and 75.4 MHz for ^{13}C on a Varian Mercury 300 spectrometer. The low-resolution mass spectrum was recorded at 20 eV on a Hewlett-Packard 5989A spectrometer, while the high-resolution mass spectrum was measured at the UCR Mass Spectrometry Facility, University of California, Riverside. Column chromatography was carried out on Merck silica gel 60 (230−400 mesh ASTM) and TLC on Merck silica gel 60 F_{254} plates. VCD and IR measurements were performed on a dualPEM Chiral*IR* FT-VCD spectrophotometer at BioTools, Inc. (Jupiter, FL). A sample of **1** (10 mg) was dissolved in CCl_4 (200 μL) and placed in a BaF_2 cell with a path length of 100 μm. Data were acquired at a resolution of 4 cm^{-1} during 9 h. The X-ray analysis was carried out on a Bruker-Nonius CAD4 diffractometer with Cu Kα radiation.

Molecular Modeling. Geometry optimizations for (+)-verticillol **1** were carried out using the MMFF94 force-field calculations as implemented in the Spartan '04 program. The systematic conformational search for the macrocycle was achieved with the aid of Dreiding models considering torsion angle movements of ca. 60°. The E_{MMFF} values were used as the convergence criterion, and a further search with the Monte Carlo protocol[32] was carried without considering an energy cutoff. A total of six minimum energy structures were found, which were optimized by DFT[20] at the B3LYP/6-31G(d,p) level of theory using the Spartan '04 routines. Gaussian 03W was used for geometry optimization of verticillane derivatives, for calculations of the IR and VCD frequencies at the B3LYP/6-31G(d,p) and B3LYP/DGDZVP levels of theory at 298 K and 1 atm, and for calculation of the electronic CD data of **8** and of the optical rotations of **1**−**8**. No solvent effects were included in the calculations, and intermolecular H-bonding interactions were not taken into consideration due to the tertiary nature of the hydroxyl group of **1**. The B3LYP/6-31G(d,p) calculations required between 60 and 65 h of computational time per conformer when using a desktop personal computer with 2 Gb RAM operated at 3 GHz, while B3LYP/DGDZVP calculations required in addition some 50 h. The empirically parametrized Altona equation was used to calculate vicinal ^{1}H NMR coupling constants from dihedral angles of each conformer.[24,25]

(1*S*,3*S*,4*S*,7*S*,8*S*,11*S*,12*R*)-(+)-3,4:7,8-Diepoxiverticillan-12-ol (4). A stirred solution of (1*S*,11*S*,12*R*)-(+)-verticilla-3*E*,7*E*-dien-12-ol (**3**)[3] (30 mg) in Bu^{t}OH (5 mL) was heated to 50 °C and treated with 30% H_2O_2 (5 mL) and SeO_2 (40 mg) during 2 h. The mixture was poured over ice−H_2O and extracted with CH_2Cl_2. The organic layer was washed with an aqueous saturated $(NH_4)_2SO_4$ (× 4) solution and H_2O (× 2), dried over anhydrous Na_2SO_4, filtered, and evaporated under vacuum. The residue was chromatographed over silica gel eluting with 1:1 CH_2Cl_2−hexane to yield compound **4** (27 mg, 81%) as a white

solid. Recrystallization from $CHCl_3$−hexane gave white needles: mp 176−178 °C; $[\alpha]_{589}$ +36, $[\alpha]_{578}$ +37, $[\alpha]_{546}$ +43, $[\alpha]_{436}$ +76, $[\alpha]_{365}$ +131, (*c* 1.05, $CHCl_3$); IR (CCl_4) ν_{max} 1462, 1450, 1385, 1371, 1159, 1088, 1067, 1057, 932, 908, 885 cm^{-1}; ^1H NMR ($CDCl_3$, 300 MHz) δ 3.21 (1H, dd, J = 7.0 and 4.8 Hz, H-3), 2.65 (1H, d, J = 8.5 Hz, H-7), 2.34 (1H, m, H-5β), 2.31 (1H, m, H-14β), 2.19 (1H, dt, J = 13.7 and 3.8 Hz, H-9α), 2.00 (1H, br dd, J = 15.6 and 7.0 Hz, H-6β), 1.86 (1H, m, H-2α), 1.86 (1H, m, H-2β), 1.82 (1H, m, H-13α), 1.76 (1H, ddd, J = 15.6, 8.0 and 4.0 Hz, H-10α), 1.66 (1H, m, H-1), 1.62 (1H, m, H-13β), 1.58 (1H, m, H-6α), 1.55 (1H, m, H-14α), 1.52 (1H, m, H-10β), 1.41 (1H, br d, J = 8.2 Hz, H-11), 1.33 (3H, s, H-19), 1.28 (1H, m, H-5α), 1.28 (3H, s, H-20), 1.25 (1H, m, H-9β), 1.19 (3H, s, H-18), 1.04 (3H, s, H-16), 0.94 (3H, s, H-17); ^{13}C NMR ($CDCl_3$, 75.4 MHz) δ 72.8 (C-12), 66.4 (C-7), 64.3 (C-3), 63.0 (C-4), 61.5 (C-8), 45.4 (C-11), 42.7 (C-1), 40.0 (C-9), 39.0 (C-13), 38.1 (C-5), 36.7 (C-15), 34.6 (C-2), 32.9 (C-18), 30.5 (C-17), 26.2 (C-14), 25.3 (C-16), 23.8 (C-6), 20.5 (C-10), 16.8 (C-19), 15.9 (C-20); CIMS (CH_3CN) *m*/*z* 377 [M + $H_2C{=}C{=}N^+{=}CH_2]^+$ (6),[33] 334 (7), 305 (54), 287 (66), 270 (100), 229 (40), 213 (33), 199 (22), 177 (26), 161 (40), 149 (63), 135 (30), 109 (32), 81 (17), 67 (26); HRCIMS (NH_3) *m*/*z* 323.2583 (calcd for $C_{20}H_{34}O_2$+H, 323.2586).

Crystal Data for 4. A crystal (0.30 × 0.30 × 0.24 mm) was obtained from $CHCl_3$−hexane. It was orthorhombic, space group $P2_12_12_1$, with cell dimensions a = 8.416(3) Å, b = 13.214(2) Å, c = 17.002(1) Å, V = 1890.8(7) $Å^3$, ρ_{calcd} = 1.133 g/cm^3 for Z = 4, MW = 322.47, and $F(000)$ = 712. The intensity data were measured using Cu Kα radiation (λ = 1.54184 Å). Reflections, measured at 296 K within a 2θ range of 4.24−59.82°, were corrected for background, Lorentz polarization, and absorption (μ = 0.578 mm^{-1}), while crystal decay was negligible. The structure was solved by direct methods using the SHELXS97 program.[34] For the structural refinement, the non-hydrogen atoms were treated anisotropically, and the hydrogen atoms, included in the structure factor calculation, were refined isotropically. The final discrepancy index was R_F = 5.0% using a unit weight for 1511 reflections and refining 229 parameters. The final difference Fourier map was essentially featureless, the highest residual peaks having densities of 0.250 e/A^3. Crystallographic data for **4** are deposited (CCDC deposition number 645788) with the Cambridge Crystallographic Data Centre. Copies of the data can be obtained, free of charge, on application to the Director, CCDC, 12 Union Road, Cambridge CB2 1EZ, UK. Fax: +44-(0)1223-336033 or e-mail: deposit@ccdc.cam.ac.uk.

Acknowledgment. We thank CONACYT-Mexico for partial financial support.

Supporting Information Available: DFT-calculated atomic Cartesian coordinates for the six conformers of **1** and X-ray atomic coordinates for **4**. Theoretical and experimental Boltzmann-weighted IR spectrum of **1**. This material is available free of charge via the Internet at http://pubs.acs.org.

References and Notes

(1) Jin, Y.; Williams, D. C.; Croteau, R.; Coates, R. M. *J. Am. Chem. Soc.* **2005**, *127*, 7834−7842.
(2) Karlsson, B.; Pilotti, A. M.; Söderholm, A. C.; Norin, T.; Sundin, S. *Tetrahedron* **1978**, *34*, 2349−2354.
(3) Hernández-Hernández, J. D.; Román-Marín, L. U.; Cerda-García-Rojas, C. M.; Joseph-Nathan, P. *J. Nat. Prod.* **2005**, *68*, 1598−1602.
(4) Duh, C. Y.; El-Gamal, A. A. H.; Wang, S. K.; Dai, C. F. *J. Nat. Prod.* **2002**, *65*, 1429−1433.
(5) Nagashima, F.; Tamada, A.; Fujii, N.; Asakawa, Y. *Phytochemistry* **1997**, *46*, 1203−1208.
(6) Nagashima, F.; Kishi, K.; Hamada, Y.; Takaoka, S.; Asakawa, Y. *Phytochemistry* **2005**, *66*, 1662−1670.
(7) Renzulli, M. L.; Rocheblave. L.; Avramova, S.; Corelli, F.; Botta, M. *Tetrahedron Lett.* **2004**, *45*, 5155−5158.
(8) Freedman, T. B.; Cao, X.; Dukor, R. K.; Nafie, L. A. *Chirality* **2003**, *15*, 743−758.
(9) Stephens, P. J.; McCann, D. M.; Devlin, F. J.; Flood, T. C.; Batkus, E.; Stončius, S.; Cheeseman, J. R. *J. Org. Chem.* **2005**, *70*, 3903−3913.
(10) Cerè, V.; Peri, F.; Pollicino, S.; Ricci, A.; Devlin, F. J.; Stephens, P. J.; Gasparrini, F.; Rompietti, R.; Villani, C. *J. Org. Chem.* **2005**, *70*, 664−669.
(11) Kuppens, T.; Vandyck, K.; Van der Eycken, J.; Herrebout, W.; van der Veken, B. J.; Bultinck, P. *J. Org. Chem.* **2005**, *70*, 9103−9114.
(12) Bouř, P.; Navrátilová, H.; Setnička, V.; Urbanová, M.; Volka, K. *J. Org. Chem.* **2002**, *67*, 161−168.
(13) Wang, F.; Wang, H.; Polavarapu, P. L.; Rizzo, C. J. *J. Org. Chem.* **2001**, *66*, 3507−3512.
(14) Nieman, J. A.; Keay, B. A.; Kubicki, M.; Yang, D.; Rauk, A.; Tsankov, D.; Wieser, H. *J. Org. Chem.* **1995**, *60*, 1918−1919.
(15) Lassen, P. R.; Skytte, D. M.; Hemmingsen, L.; Nielsen, S. F.; Freedman, T. B.; Nafie, L. A.; Christensen, S. B. *J. Nat. Prod.* **2005**, *68*, 1603−1609.
(16) Monde, K.; Taniguchi, T.; Miura, N.; Kutschy, P.; Čurillová, Z.; Pilátová, M.; Mojžiš, J. *Bioorg. Med. Chem.* **2005**, *13*, 5206−5212.
(17) Cichewicz, R. H.; Clifford, L. J.; Lassen, P. R.; Cao, X.; Freedman, T. B.; Nafie, L. A.; Deschamps, J. D.; Kenyon, V. A.; Flanary, J. R.; Holman, T. R.; Crews, P. *Bioorg. Med. Chem.* **2005**, *13*, 5600−5612.
(18) Muñoz, M. A.; Muñoz, O.; Joseph-Nathan, P. *J. Nat. Prod.* **2006**, *69*, 1335−1340.
(19) Stephens, P. J.; Pan, J. J.; Devlin, F. J.; Urbanová, M.; Hájíček, J. *J. Org. Chem.* **2007**, *72*, 2508−2524.
(20) Perdew, J. P. *Phys. Rev. B* **1986**, *33*, 8822−8824.
(21) Kolossváry, I.; Guida, W. C. *J. Am. Chem. Soc.* **1993**, *115*, 2107−2119.
(22) Christensen, I. T.; Jørgensen, F. S. *J. Comput. Aided Mol. Des.* **1997**, *11*, 385−394.
(23) Furo, T.; Mori, T.; Wada, T.; Inoue, Y. *J. Am. Chem. Soc.* **2005**, *127*, 8242−8243.
(24) Haasnoot, C. A. G.; de Leeuw, F. A. A. M.; Altona, C. *Tetrahedron* **1980**, *36*, 2783−2792.
(25) Cerda-García-Rojas, C. M.; Zepeda, L. G.; Joseph-Nathan, P. *Tetrahedron Comp. Methodol.* **1990**, *3*, 113−118.
(26) Pereda-Miranda, R.; Fragoso-Serrano, M.; Cerda-García-Rojas, C. M. *Tetrahedron* **2001**, *57*, 47−53.
(27) Drawings have been modified with respect to the original papers to be consistent with the absolute configuration revision.
(28) Lightner, D. A. In *Circular Dichroism-Principles and Applications*; Berova, N., Nakanishi, K., Woody, R. W., Eds.; Wiley-VCH: New York, 2000, pp 261−303.
(29) Lightner, D. A.; Chang, T. C.; Hefelfinger, D. T.; Jackman, D. E.; Wijekoon, W. M. D.; Givens, J. W., III. *J. Am. Chem. Soc.* **1985**, *107*, 7499−7508.
(30) Lightner, D. A.; Gurst, J. E. *Organic Conformational Analysis and Stereochemistry from Circular Dichroism Spectroscopy*; Wiley-VCH: New York, 2000; pp 56−61.
(31) Stephens, P. J.; McCann, D. M.; Devlin, F. J.; Smith, A. B., III. *J. Nat. Prod.* **2006**, *69*, 1055−1064.
(32) Chang, G.; Guida, W. C.; Still, W. C. *J. Am. Chem. Soc.* **1989**, *111*, 4379−4386.
(33) In analogy to known cases. See: Lawrence, P.; Brenna, J. T. *Anal. Chem.* **2006**, *78*, 1312−1317.
(34) Sheldrick, G. M. *Programs for Crystal Structure Analysis*; Institut für Anorganische Chemie der Universität: Göttingen, Germany, 1998.

NP0605992